

ROBUST UNSUPERVISED MULTI-OBJECT TRACKING IN NOISY ENVIRONMENTS

C.-H. Huck Yang^{1†}, Mohit Chhabra², Y.-C. Liu¹, Quan Kong², Tomoaki Yoshinaga², Tomokazu Murakami²

¹Georgia Institute of Technology, Atlanta, GA, USA
²Lumada Data Science Lab. Hitachi, Ltd., Tokyo, Japan

ABSTRACT

Physical processes, camera movement, and unpredictable environmental conditions like the presence of dust can induce noise and artifacts in video feeds. We observe that popular unsupervised MOT methods are dependent on noise-free inputs. We show that the addition of a small amount of artificial random noise causes a sharp degradation in model performance on benchmark metrics. We resolve this problem by introducing a robust unsupervised multi-object tracking (MOT) model: AttU-Net. The proposed single-head attention model helps limit the negative impact of noise by learning visual representations at different segment scales. AttU-Net shows better unsupervised MOT tracking performance over variational inference-based state-of-the-art baselines. We evaluate our method in the MNIST-MOT and the Atari game video benchmark. We also provide two extended video datasets: “Kuzushiji-MNIST MOT” which consists of moving Japanese characters and “Fashion-MNIST MOT” to validate the effectiveness of the MOT models.

Index Terms— Multi-object tracking, Unsupervised learning, Video tracking, Robust representation learning.

1. INTRODUCTION

Multi-object tracking (MOT) is a challenging video processing task, where the aim is to locate and track one or more visual pattern(s) from an input video. MOT has many essential real-world applications, such as multimedia content analysis [1] and industrial automation [2]. However, the time and pecuniary cost of labeling large-scale video data constrains the effectiveness of current methods. Unsupervised Multi-Object Tracking (UMOT) is an appealing approach to further improve performance without the requirement of labeled training data.

Real-world applications often require data processing in the presence of **environmental noise** as shown in Figure 1 which is different from UMOT evaluations of video data in carefully controlled laboratory settings. The robustness of

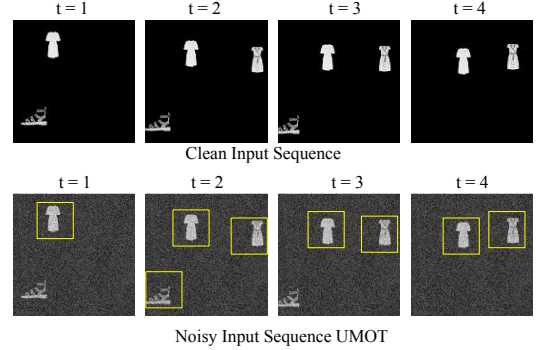


Fig. 1: Unsupervised Multi-Object Tracking (UMOT) results on Fashion-MNIST MOT dataset based on Fashion-MNIST [6]. Experimental setup is motivated by [3, 7].

UMOT performance against environmental noise also remains relatively unexplored. In this work, we first evaluate the robustness of the state-of-the-art UMOT model against artificial noise. We propose a multi-scale tracker based on attention U-Net to improve model generalization and to avoid over-fitting on background pixels. We also show ablation studies on different visual and optimization setups in the MNIST-MOT benchmark and two extended video datasets. Our contributions include:

- Investigation of the effect of noise on UMOT performance.
- A new DNN video tracking backbone to leverage upon attention U-Net for robust UMOT.
- Evaluation of the proposed method on MNIST-MOT [3], Atari gaming video [4], and two newly created UMOT datasets with complex patterns: (1) Kuzushiji-MNIST MOT derived from [5] and (2) Fashion-MNIST MOT derived from [6].

2. RELATED WORK

2.1. Unsupervised Multi-Object Tracking

Unsupervised object tracking often incorporates visual reconstruction and geometric rendering to utilize spatial information for predicting bounding boxes. Tracking by anima-

[†]A part of this work was done during Huck’s visit to Hitachi Central Research Lab, Tokyo, Japan. Datasets are available at <https://github.com/huckiyang/MOT-Kuzushiji-Fashion-Video>.

tion [3] (TBA) showed the first competitive UMOT results on both the MNIST-MOT and DukeMTMC [8] dataset. It used a recurrent neural network (RNN) to learn the representations of object motion and a convolutional neural network (CNN) based autoencoder to reconstruct frames and visual patterns from geometrical tracker arrays. Spatially invariant attend-infer-repeat (SPAIR) models [7] used CNN feature extractors and a local spatial object specification scheme to conduct UMOT video processing with variational inference. Building upon the SPAIR method, spatially invariant label-free object tracking (SILOT) [4] incorporated VAE based architecture with competitive MOT accuracy on MNIST-MOT and Atari video games. However, previous methods and benchmark models do not provide experimental studies on the effect of background noise on tracker performance. This motivates the evaluation setup under noisy conditions.

2.2. Self attention for robustness

Image denoising [9] with the objective of image enhancement has been studied extensively in the literature (e.g., image dehazing [10]). Image de-noising approaches have also been investigated in the context of improving representation learning. U-Net [11] was initially introduced for the task of biomedical image segmentation with few labeled images. U-Net based multi-scale learning architectures, such as Wave-U-Net [12] and attention U-Nets [13, 14], have attained competitive results against noisy inputs by learning across multiple scales over input segments. Siam-U-Net [15] has shown that U-Net based encoders perform well on visual tracking tasks. In this work, we build upon U-Net based backbone for UMOT. The motivation is to enhance model generalization with multi-scale de-noising.

3. ENHANCED UNSUPERVISED MULTI-OBJECT TRACKING

3.1. Noisy Background Setup

The loss function l_t at time t is defined similarly to the loss function in TBA (refer to Eq. (9) in [3]):

$$l_t = \text{MSE}(\mathbf{X}_t, \mathbf{X}_t^C) + \lambda \cdot \frac{1}{I} \sum_{i=1}^4 (s_{t,i}^x, s_{t,i}^y), \quad (1)$$

where the first term is the mean squared error (MSE) between \mathbf{X}_t , a ground truth frame and \mathbf{X}_t^C , reconstructed frame generated by DNN. The second term is tightness constraint on the bounding box size and is computed by λ , a scaling coefficient; I , the number of trackers and $s_{t,i}^x, s_{t,i}^y$ object poses.

To simulate noisy conditions, we consider random noise $\delta_t \sim \mathcal{N}(0, 1)$ sampled from Gaussian distribution, which has been used previously in robust video learning studies [16, 17, 2]. The total training frames of a video input in Eq. (1) are modified to $\sum_{t=1}^T \mathbf{X}'_t = \sum_{t=1}^T (\mathbf{X}_t + \beta \times \delta_t)$ as a **noisy**

setup in testing for total time step $t \in \{1, 2, \dots, T\}$, where $\beta \in \{0\%, 10\%, 20\%, 30\%\}$ scales the noise magnitude to a percentage of maximum intensity (refer to [16, 17]).

3.2. Attention U-Net Feature Encoder

We design a spatial feature encoder consisting of transformer-based single-head attention [18, 19] module. ResNet₁₈ [20] encoder extracts the features map (m_t) from inputs \mathbf{X}_t . The feature map m_t is also used to extract key k_t , value (v_t) and query (q_t) tensors. The attention map (A_t) is computed by scaling the value (v_t) tensor by the inner product of the key (k_t) and query (q_t) tensors along the spatial dimensions (width and height) of the feature map. Here, the view operation is used to reshape the tensors.

$$m_t = f_{ResNet, \theta_1}(\mathbf{X}_t); \quad q_t = \text{view}(f_{q, \theta_2}(m_t)); \quad (2)$$

$$k_t = \text{view}(f_{k, \theta_3}(m_t)); \quad v_t = \text{view}(f_{v, \theta_4}(m_t)); \quad (3)$$

$$A_t = \text{view}\left(\frac{q_t k_t^T}{\sqrt{d_k}}\right) v_t, \quad (4)$$

where $f_{ResNet}, f_q, f_k, f_v$ are individual DNNs with hyperparameters (θ_1 to θ_4) updated by end-to-end gradient descent training. As shown in Figure 2 (a), a U-Net [11] encoder is used to learn multi-scale features from the attention map: $C_t = \text{U-Net}(A_t; \theta_5)$. The attention U-Net comprises of channel sizes $\{32, 64, 128, 64, 32\}$. Each convolutional layer is followed by a rectified linear unit and a 2×2 max-pooling operation with stride 2 for down-sampling.

3.3. Tracker Arrays and Rendering

After obtaining the feature representation C_t , we use tracker arrays to extract the individual location of the object(s) from a frame. As shown in Figure 2 (b), we use a latent state $\mathbf{H}_{(t,i)}$ feature extractor for i^{th} tracker to convert spatial information by neural sequence modeling:

$$\mathbf{H}_{(t,i)} = f_{seq, \theta_6}(\mathbf{H}_{t-1}, C_t), \quad (5)$$

where f_{seq, θ_6} consists of bidirectional GRU [21] networks. To obtain the location of objects in an unsupervised manner, we incentivize a jointly parameterized tracker network (f_{joint}) to predict a single object location ($\mathbf{Y}_{t,i}$).

$$\mathbf{Y}_{t,i} = f_{\text{joint}}(\mathbf{h}_{t,i}; \boldsymbol{\theta}^{\text{out}}) \quad (6)$$

where the output $\mathbf{Y}_{t,i}$ is a mid-level representation of objects on 2D image planes, including: (a) probability of having tracked an object; (b) object pose ($s_{t,i}^x, s_{t,i}^y$ in Eq. (1)); (c) shape (with channel size); (d) object appearance. These mid-level output locations are used to validate model performance by MOT evaluation. We follow the layer-wise composition setup from TBA [3] and use Spatial Transformer Network (STN) [22] to scale $\mathbf{Y}_{t,i}$ to multiple layer foreground (L_t^k)

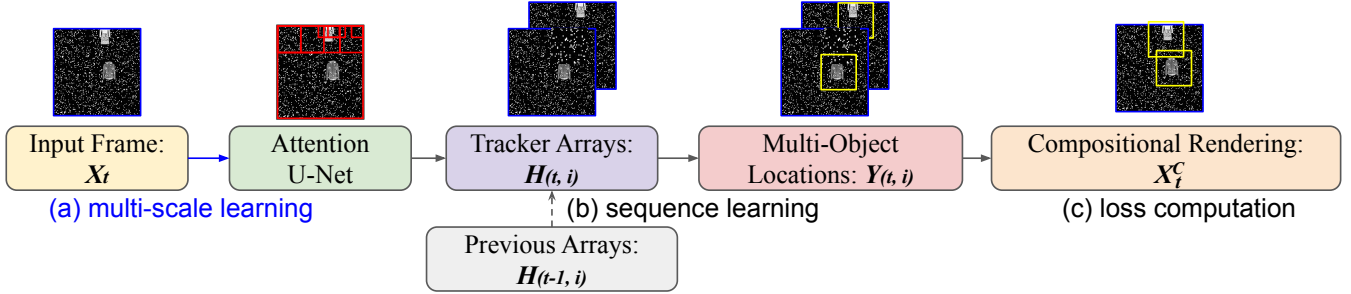


Fig. 2: Overview of the U-Net enhanced animation tracking framework: (a) multi-scale learning; (b) sequence learning; (c) loss computation. This enhanced scale-free learning method is motivated by the tracking-by-animation benchmark [3].

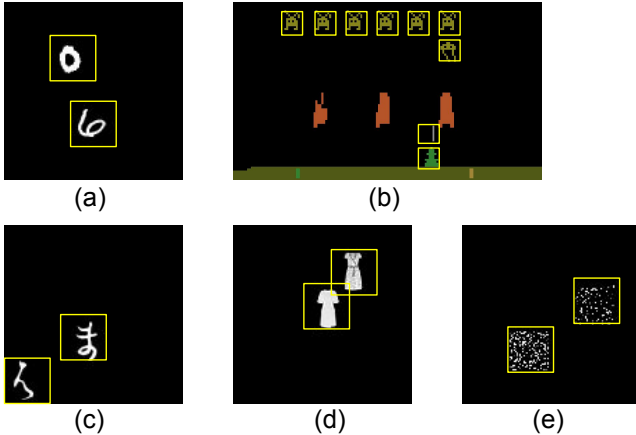


Fig. 3: Four training datasets used in our experiments: (a) MNIST-MOT [3, 7], (b) Atari gaming video [4], (c) Kuzushiji-MNIST MOT, and (d) Fashion-MNIST MOT. A test dataset with scrambled objects (e) is also provided to evaluate generalization ability.

and layer masks ($L-m_t^k$) with layer number $k = 3$. As shown in Figure 2 (c), we contain the DNN reconstructed frame X_t^C by using layer-wise geometrical composition:

$$X_t^{(k)} = (1 - L-m_t^k) \odot X_t^{(k-1)} + L_t^k; \quad (7)$$

$$X_t^C = \sum_{k=1}^3 X_t^{(k)}, \quad (8)$$

X_t^C is used for computing reconstruction loss Eq. (1).

4. EXPERIMENTS

4.1. Datasets and Baseline Setup

As shown in Figure 3, we select two baseline video datasets from the previous UMOT studies: (a) MNIST-MOT [3, 7] containing $2M$ training frames and $25k$ validation frames, where each frame is of size $128 \times 128 \times 1$ and (b) Atari gaming video on Space-Invader (Atari-SI) [4, 7] containing $128k$ training frames and $1k$ validation frames, where each frame is converted to gray-scale with a input size of $210 \times 160 \times 1$ for testing.

MOT Video Datasets: To study the effects of tracking on patterns other than MNIST characters, we provide two new MOT video datasets with more intricate patterns (c) Japanese cursive characters (denoted as **Kuzushiji** from [5]) and (d) Fashion-MNIST MOT (denoted as **Fashion** derived from [6]). These new datasets have been chosen to study complex visual patterns and could be useful for different UMOT applications (e.g., pedestrian tracking).

Object-Scrambling Test: To verify whether the unsupervised model indeed learns semantically meaningful patterns, we provide an **object-scrambling** video test-set containing $1k$ frames as shown in Figure 3 (e). The test-set was constructed from the MNIST-MOT video dataset by randomly permuting the pixels in object bounding boxes. Ideally, a robust UMOT model [7, 2] should learn semantically consistent discriminative representations for predicting object location. A model which learns such discriminative patterns on the MNIST-MOT dataset is expected to have degraded performance on the object scramble test-set.

Baseline Models: We select two major benchmark UMOT models as reproducible studies as shown in Table 1.

- Tracking by animation (TBA) [3]: a model combines with RNNs for sequence modeling with attention features and uses CNN feature extraction for representation learning on frame rendering.
- Spatially invariant label-free object tracking (SILOT) [4]: a model built upon VAE for frame-wise reconstruction and using YOLO-based CNN feature extraction for representation learning.

U-Net based UMOT backbones: We design two different type of U-Net based feature encoder backbones: residual U-Net network with a ResNet₅₀ encoder (denoted as **ResU-Net**) and propose self-attention U-Net (denoted as **AttU-Net**) as discussed in section 3.2. The tested UMOT models have a comparable number of model parameters $\sim 12M$.

4.2. UMOT Performance in Different Contexts

As shown in Figure 4, we evaluated the MOT accuracy with noise level ranging from 0% (without noise) to 30%. All the models were trained by using noise free frames as shown

Table 1: Detailed MOT metrics in the clean MNIST-MOT dataset [3, 4] with UMOT models as a reproducible baseline.

Model	IDF1	IDP	IDR	RcII	Prcn	GT	MT	PT	ML	FP	FN	IDs	FM	MOTA	MOTP
TBA	99.4%	99.3%	99.5%	99.8%	99.6%	99	99	2	0	9	4	2	1	99.3%	88.4%
SILOT	98.9%	98.2%	99.5%	99.9%	98.5%	100	100	0	0	34	3	7	1	98.0%	85.9%
ResU-Net	99.5%	99.5%	99.8%	100.0%	99.7%	99	99	0	4	3	2	1	0	99.4%	89.2%
AttU-Net	99.9%	99.9%	100.0%	100.0%	99.9%	99	99	0	0	3	1	1	0	99.8%	89.6%

in Figure 3 (a) to (d). In the noise free setting (0% noise), MNIST-MOT derived from (4a) and Kuzushiji-MOT derived from (4c), the evaluated models attained MOT accuracy ranging above 95; Atari-SI (4b) and Fashion-MNIST MOT derived from (4d) were found to be more challenging and the MOT accuracy was below 90% for tested models. When the noise magnitude was increased, TBA model showed a sharp decrease in performance over all tested datasets. MOT accuracy for TBA model fell below $\sim 20\%$ in the MNIST-MOT dataset as noise was increased to 30%.

Although SILOT models are more robust than TBA under the presence of small amount of noise. Their performance suffers major degradation when the noise ratio is increased. It decreases to 52.12% in Atari-SI when the noise level is 20%. For U-Net based backbones, both ResU-Net and AttU-Net show robustness in the MNIST-MOT dataset even with the presence 30% noise. For all datasets, AttU-Net based UMOTs show best performance with substantial absolute improvements ($\sim 3\text{-}5\%$) over the ResU-Net with the exception of Fashion-MNIST MOT where the improvement is (1.01%) as (4d). In short, the performance of existing benchmark UMOTs, TBA and SILOT, are sensitive to noise whereas U-Net based UMOTs perform competitively.

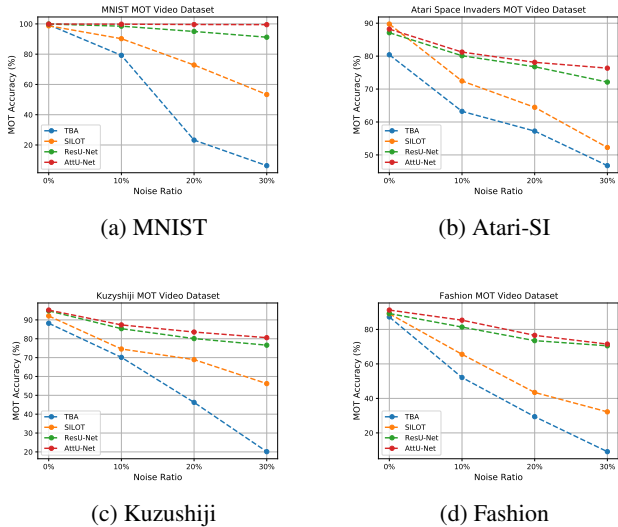


Fig. 4: MOTA Performance under different noisy level testing in: (a) MNIST-MOT [7, 3], (b) Atari-Space Invader [4] (SI) video, (c) Kuzushiji-MNIST MOT, and (d) Fashion-MNIST MOT tracking datasets.

4.3. Evaluation of UMOT Model Generalization

To study generalization of different UMOT models with noisy inputs, we evaluated pre-trained UMOT models on MNIST-MOT test set in two different configurations. **(1) Testing with scrambled objects:** As in Table 2, U-Net backbones show major degradation when context-wise representation has been corrupted by the scrambled object settings (S). As discussed in Section 4.1 U-Net backbones generalize better than baseline models. **(2) Training with augmented noise:** We also evaluated as to how models would benefit from training with noisy Fashion-MNIST MOT video dataset. As shown in Table 3, both U-Net based UMOT models show better performance than TBA and SILOT by a noisy training (N) with augmented inputs containing 30% noise ratio. All UMOTs improve in terms of absolute performance but the architecture-specific (e.g., multi-scale learning by U-Net based backbones) differences still significantly impact performance metrics.

Table 2: Performance of pretrained UMOT models on MNIST-MOT when tested on scrambled MNIST objects (S). Higher numbers indicates lack of semantic context.

	TBA [3]	SILOT [4]	ResU-Net	AttU-Net
S -MOTA	91.4%	83.9%	65.1%	61.7%
S -MOTP	90.9%	82.1%	61.4%	59.8%

Table 3: Performance of different UMOT models trained with 30% noise (N) in Fashion-MNIST MOT dataset. Higher numbers indicate better generalisation ability.

	TBA [3]	SILOT [4]	ResU-Net	AttU-Net
N -MOTA	24.1%	46.7%	76.3%	81.2%
N -MOTP	23.2%	44.8%	75.2%	80.1%

5. CONCLUSION

In this work, we studied UMOT performance with noisy inputs and show that pre-existing methods suffer a substantial decrease in MOT accuracy when the noise ratio is increased above 30%. AttU-Net based approach increases the robustness to noise on all evaluated data sets. We also show the ability of AttU-Net to learn semantically relevant features by testing it on the test set of scrambled instances.

6. REFERENCES

- [1] Anders Johansson, Dirk Helbing, and Pradyumn K Shukla, "Specification of the social force pedestrian model by evolutionary adjustment to video tracking data," *Advances in complex systems*, vol. 10, no. supp02, pp. 271–288, 2007.
- [2] Sorin Grigorescu, Bogdan Trasnea, Tiberiu Cocias, and Gigel Macesanu, "A survey of deep learning techniques for autonomous driving," *Journal of Field Robotics*, vol. 37, no. 3, pp. 362–386, 2020.
- [3] Zhen He, Jian Li, Daxue Liu, Hangen He, and David Barber, "Tracking by animation: Unsupervised learning of multi-object attentive trackers," in *Proceedings of the IEEE Conference on Computer Vision and Pattern Recognition*, 2019, pp. 1318–1327.
- [4] Eric Crawford and Joelle Pineau, "Exploiting spatial invariance for scalable unsupervised object tracking," in *Proceedings of the AAAI Conference on Artificial Intelligence*, 2020, vol. 34, pp. 3684–3692.
- [5] Tarin Clanuwat and et al., "Deep learning for classical japanese literature," *arXiv preprint arXiv:1812.01718*, 2018.
- [6] Han Xiao and et al., "Fashion-mnist: a novel image dataset for benchmarking machine learning algorithms," *arXiv preprint arXiv:1708.07747*, 2017.
- [7] Eric Crawford and Joelle Pineau, "Spatially invariant unsupervised object detection with convolutional neural networks," in *Proceedings of the AAAI Conference on Artificial Intelligence*, 2019, vol. 33, pp. 3412–3420.
- [8] Mengran Gou and et al., "Dukemtmc4reid: A large-scale multi-camera person re-identification dataset," in *Proc. CVPR Workshops*, 2017, pp. 10–19.
- [9] Antoni Buades, Bartomeu Coll, and Jean-Michel Morel, "A review of image denoising algorithms, with a new one," *Multiscale Modeling & Simulation*, vol. 4, no. 2, pp. 490–530, 2005.
- [10] Hao-Hsiang Yang, Chao-Han Huck Yang, and Yi-Chang James Tsai, "Y-net: Multi-scale feature aggregation network with wavelet structure similarity loss function for single image dehazing," in *2020 IEEE International Conference on Acoustics, Speech and Signal Processing (ICASSP)*. IEEE, 2020, pp. 2628–2632.
- [11] Olaf Ronneberger, Philipp Fischer, and Thomas Brox, "U-net: Convolutional networks for biomedical image segmentation," in *International Conference on Medical image computing and computer-assisted intervention*. Springer, 2015, pp. 234–241.
- [12] Hao-Hsiang Yang and Yanwei Fu, "Wavelet u-net and the chromatic adaptation transform for single image dehazing," in *2019 IEEE International Conference on Image Processing (ICIP)*. IEEE, 2019, pp. 2736–2740.
- [13] Ozan Oktay and et al., "Attention u-net: Learning where to look for the pancreas," *arXiv preprint arXiv:1804.03999*, 2018.
- [14] Hao-Hsiang Yang, Chao-Han Huck Yang, and Yu-Chiang Frank Wang, "Wavelet channel attention module with a fusion network for single image deraining," in *2020 IEEE International Conference on Image Processing (ICIP)*. IEEE, 2020, pp. 883–887.
- [15] Matteo et al. Dunnhofer, "Siam-u-net: encoder-decoder siamese network for knee cartilage tracking in ultrasound images," *Medical Image Analysis*, vol. 60, pp. 101631, 2020.
- [16] Chao-Han Huck Yang, Jun Qi, Pin-Yu Chen, Yi Ouyang, I-Te Danny Hung, Chin-Hui Lee, and Xiaoli Ma, "Enhanced adversarial strategically-timed attacks against deep reinforcement learning," in *2020 IEEE International Conference on Acoustics, Speech and Signal Processing (ICASSP)*. IEEE, 2020, pp. 3407–3411.
- [17] Yen-Chen Lin and et al., "Tactics of adversarial attack on deep reinforcement learning agents," in *Proceedings of the 26th International Joint Conference on Artificial Intelligence*, 2017, pp. 3756–3762.
- [18] Chao-Han Yang, Jun Qi, Pin-Yu Chen, Xiaoli Ma, and Chin-Hui Lee, "Characterizing speech adversarial examples using self-attention u-net enhancement," in *2020 IEEE International Conference on Acoustics, Speech and Signal Processing (ICASSP)*. IEEE, 2020, pp. 3107–3111.
- [19] Ashish Vaswani and et al., "Attention is all you need," *Advances in Neural Information Processing Systems*, vol. 30, pp. 5998–6008, 2017.
- [20] Kaiming He, Xiangyu Zhang, Shaoqing Ren, and Jian Sun, "Deep residual learning for image recognition," in *Proceedings of the IEEE conference on computer vision and pattern recognition*, 2016, pp. 770–778.
- [21] Junyoung Chung, Caglar Gulcehre, KyungHyun Cho, and Yoshua Bengio, "Empirical evaluation of gated recurrent neural networks on sequence modeling," *arXiv preprint arXiv:1412.3555*, 2014.
- [22] Max Jaderberg, Karen Simonyan, Andrew Zisserman, et al., "Spatial transformer networks," *Advances in neural information processing systems*, vol. 28, pp. 2017–2025, 2015.